Biogeochemistry
https://doi.org/10.1007/s10533-023-01026-x

# Controls on organic and inorganic soil carbon in poorly drained agricultural soils with subsurface drainage

**Wenjuan Huang · Anthony J. Mirabito · Carlos G. Tenesaca · William F. Mejia-Garcia · Nathaniel C. Lawrence · Amy L. Kaleita · Andy VanLoocke · Steven J. Hall**

Received: 27 October 2022 / Accepted: 28 January 2023


**Abstract** Many productive agricultural soils have naturally poor drainage characteristics and may intermittently pond water even where artificial drainage infrastructure is present, especially in topographic depressions. Soil organic carbon (SOC) is often higher in depressions than uplands, but whether temporary ponding increases SOC by suppressing decomposition remains an important knowledge gap. We measured SOC and inorganic C (carbonate) along topographic gradients from tile-drained depressions to adjacent uplands and tested their relationships with hydrological and biogeochemical properties in corn/soybean fields in Iowa, USA, and examined soil respiration and its stable C isotopes ($\delta^{13}C$) by lab incubation. The 0–30 cm SOC concentration was greatest at depression bottoms, as expected, while carbonate C was highest at boundaries between depressions and uplands. However, only carbonate C, not SOC, increased in depressions with increasingly poor drainage (greater ponding duration). Silt + clay content was the strongest positive predictor of SOC, while ponding duration and oxalate-extractable iron were negatively related to SOC in a statistical model ($R^2 = 0.83$). These negative relationships are consistent with suppression of crop biomass production and iron-mediated decomposition in periodically anoxic soil. Soil C/N ratios were similar in depressions and uplands, indicating that plant detritus did not accumulate with ponding. Stable C isotopes of respiration from incubated soils indicated a similar $C_3/C_4$ plant mixture in depressions and uplands, consistent with decomposing soybean and corn residues. In contrast, depression soil organic matter had lower $\delta^{13}C$ and $\delta^{15}N$ values than uplands, more consistent with pre-agricultural prairie plants than crop residues. Accumulation of SOC in these agricultural depressions is more likely explained by erosion than by suppression of decomposition due to temporary ponding. Gaining additional SOC may require fundamental changes in management, or wetland restoration.

Responsible Editor: Edith Bai.

**Supplementary Information** The online version contains supplementary material available at https://doi.org/10.1007/s10533-023-01026-x.

W. Huang · A. J. Mirabito · C. G. Tenesaca · W. F. Mejia-Garcia · N. C. Lawrence · S. J. Hall (✉)
Department of Ecology, Evolution, and Organismal Biology, Iowa State University, Ames, IA, USA
e-mail: stevenjh@iastate.edu

A. J. Mirabito
Department of Biology, University of Central Florida, Orlando, FL, USA

A. L. Kaleita
Department of Agricultural and Biosystems Engineering, Iowa State University, Ames, IA, USA

A. VanLoocke
Department of Agronomy, Iowa State University, Ames, IA, USA

Published online: 07 February 2023

**Keywords** Carbon stable isotope · Carbonate · $C_3$ and $C_4$ plants · Prairie pothole · Redox · Wetland

## Introduction

The high moisture content of undisturbed wetland soils may lead to sustained periods of anoxic conditions that suppress organic matter decomposition and promote soil organic carbon (SOC) accumulation (Ponnamperuma 1972) due to the kinetic and thermodynamic constraints on C depolymerization and microbial metabolism imposed by oxygen limitation. Accordingly, drainage of wetlands for agriculture has led to widespread SOC loss (Bridgham et al. 2006). At least 10% of global agricultural land has been artificially drained, including highly productive grain-cropping regions of North America and Europe (Smedema et al. 2000; Castellano et al. 2019). In the northwestern US Corn Belt region, depressional wetlands known as prairie potholes were once common but have now mostly been drained for agriculture (Van Meter and Basu 2015). We describe these former wetlands as "cropped depressions", given that they may or may not meet regulatory requirements for classification as farmed wetlands under their current drainage conditions (Schilling and Dinsmore 2018). Cropped depressions have lower SOC than natural prairie pothole wetlands, particularly at the soil surface (Euliss et al. 2006). Nevertheless, some cropped depressions still have relatively high SOC concentrations (e.g., $>50$ mg C $g^{-1}$) in surface horizons, especially compared with adjacent upland soils (James and Fenton 1993; Supplementary Fig. S1). In cropland soils with inefficient drainage infrastructure, periods of high moisture and associated anoxic conditions might continue to protect SOC from decomposition (Castellano et al. 2019). However, it is also possible that other mechanisms, such as erosion of C-rich fine particles from upslope soils (Berhe et al. 2018; Li et al. 2018), could also explain high SOC in cropped depressions. Identifying the biogeochemical predictors of SOC distribution among cropped depressions and their adjacent uplands may contribute to our fundamental understanding of SOC accrual in environments with dynamic moisture and oxygen availability (Keiluweit et al. 2017; Huang and Hall 2017; Huang et al. 2021) and could inform the management of poorly drained agroecosystems for carbon sequestration, especially in the context of rapidly developing agricultural soil carbon markets (Lorenz and Lal 2022).

Although many cropped depressions in the US Corn Belt are artificially drained by subsurface pipes known as tiles, soils may still pond water for days or weeks following large precipitation events due to low hydraulic conductivity or backup of water in downstream drains (Schilling et al. 2018; Martin et al. 2019). Ponded soils are often characterized by anoxic conditions due to restricted oxygen diffusion (Ponnamperuma 1972), and anoxic zones can also occur in wet soils that are not saturated with moisture (Silver et al. 1999), especially within soil aggregates, where biological oxygen demand may exceed supply (Sexstone et al. 1985). Previous work provided multiple lines of evidence for anoxic conditions during periods of high moisture in cropped depression soils of Iowa and Illinois, USA, including depletion of oxygen in soil pores, stimulation of denitrification, accumulation of ferrous iron due to anaerobic microbial metabolism, and accumulation of ammonium due to suppression of nitrification, an obligate aerobic process (Krichels et al. 2019; Suriyavirun et al. 2019; Yu et al. 2021; Lawrence et al. 2021). However, anoxic conditions in these cropped depressions were temporary, not consistent: when moisture decreased, macropore oxygen concentrations increased, ferrous iron was largely oxidized to ferric iron, and nitrate became the dominant form of inorganic N (Krichels et al. 2019; Suriyavirun et al. 2019; Yu et al. 2021; Lawrence et al. 2021). Furthermore, when temperatures were cold, soil respiration did not consistently deplete oxygen even when ponding occurred (Krichels and Yang 2019).

Despite evidence of intermittent anoxic conditions linked to ponding in cropped depression soils, the overall impact on SOC accrual remains unclear. On one hand, we might expect that a greater frequency or spatial extent of anoxic conditions would lead to SOC accumulation even in cases where soils do not remain consistently or completely anoxic (Hall and Silver 2015; Keiluweit et al. 2017). Consistent with this reasoning, SOC was lower in tile-drained than non-drained agricultural soils with otherwise similar characteristics (Kumar et al. 2014; Fernández et al. 2017). On the other hand, lab experiments indicated that even brief periods of oxygen availability may counteract temporary decreases in decomposition under

anoxic conditions (Reddy and Patrick 1975; Huang et al. 2021), due in part to decomposition pathways linked to iron (Fe) redox cycling. Under oxic conditions, Fe minerals can protect SOC from decomposition by forming organo-mineral associations, but during fluctuating oxic/anoxic conditions, Fe can also promote SOC decomposition via several biogeochemical mechanisms. For example, Fe oxidation can produce reactive oxygen species to directly stimulate $CO_2$ production and/or increase C availability by cleaving organic polymers during oxic periods, and Fe reduction is a favorable electron accepting process that can increase availability of C previously trapped by Fe minerals to fuel $CO_2$ production during anoxic periods; these processes can largely counteract protection of C by Fe under redox fluctuations (Huang and Hall 2017; Chen et al. 2020). Furthermore, previous field measurements in cropped depressions suggested an ambiguous impact of drainage on SOC stocks. Across the Prairie Pothole Region, depressional wetlands which had been previously farmed had similar 0–30 cm SOC stocks regardless of whether they were drained (99 Mg C $ha^{-1}$) or nondrained (96 Mg C $ha^{-1}$; Euliss et al. 2006). Similarly, SOC depth profiles were generally similar along paired catenas of Iowa agricultural soils with and without subsurface tile drainage (James and Fenton 1993; Supplementary Fig. S1). Taken together, these arguments suggest that the high SOC concentrations of cropped depressions that experience inconsistent ponding might not necessarily be related to temporary suppression of decomposition by anoxic conditions.

Soil erosion could also contribute to SOC accumulation in cropped depressions. Fine soil particles enriched in SOC are more prone to be transported from upslope to low-lying areas, and agricultural tillage has aggravated this process over many decades (Thaler et al. 2021). Li et al. (2018) used historic orthophotos and cesium ($^{137}Cs$) measurements to trace erosion and deposition in central Iowa croplands. They found that depressions had greater SOC due to redistribution of the C-rich topsoil from uplands to depressions, but suggested that greater moisture and associated anoxic conditions in depressions may also have contributed (Li et al. 2018). However, the relative influence of elevated moisture on SOC could not be directly tested in that study.

Soil inorganic C (carbonate) might be used as a longer-term metric of depression hydrology, given that carbonate leaching is strongly related to soil water flux over pedogenic timescales (Egli and Fitze 2001). Carbonate often accumulates in depressions, especially at the depression/upland interface, due to accumulation and evaporation of calcium-rich water; conversely, carbonate is generally leached from surface horizons of well-drained soils (Knuteson et al. 1989; Khan and Fenton 1994; Logsdon and James 2014). Thus, we expect that differences in carbonate C are related to differences in water balance (evaporation vs. infiltration) among depressions. If so, carbonate C could provide additional insight into relationships between ponding and SOC accrual.

Along with organic and inorganic C, stable isotope analyses of SOC, total soil N, and C in respired $CO_2$ provide additional context for organic matter dynamics. The corn–soybean rotation is the dominant cropping system across the US Corn Belt. Corn is a $C_4$ plant with typical $\delta^{13}C$ values near $-12‰$, and soybean is a $C_3$ plant with typical $\delta^{13}C$ values near $-27‰$ (Li et al. 2018; Hall et al. 2019). In corn–soybean rotations, typical $\delta^{13}C$ values of SOC and soil respiration (e.g., $-15$ to $-18‰$) reflect a mixture of these $C_3$ and $C_4$ sources, often with a larger corn contribution because of its greater residue production (Huggins et al. 1998; Russell et al. 2009; Ye and Hall 2020). Prior to row-crop agriculture, native prairie plant communities in our region were also mixtures of $C_3$ and $C_4$ species, but the SOC derived from prairie plants often had a stronger $C_3$ contribution than in comparable cropland soils, with typical $\delta^{13}C$ values $< -20‰$ at the surface (Huggins et al. 1998; Russell et al. 2009). Therefore, soils with lower $\delta^{13}C$ values in this region may indicate greater contributions of legacy prairie C vs. recent corn–soybean C to total SOC (Li et al. 2018). Soil nitrogen (N) isotopes also can provide insight into sources and transformations of soil organic matter. Agricultural soils often have higher $\delta^{15}N$ values than non-agricultural soils as a consequence of their greater N losses, which can lead to N isotope fractionation, and also due to application of manure, which has high $\delta^{15}N$ values (Choi et al. 2017). Thus, we would expect lower values of $\delta^{13}C$ and $\delta^{15}N$ in soils with greater contributions of legacy prairie-derived organic matter vs. modern sources.

To examine the spatial distribution and controls on SOC and inorganic C in cropped depressions and their adjacent uplands, here we leveraged previous multi-year measurements of surface water ponding

in cropped depressions in Iowa, USA, which differed in their drainage characteristics (Martin et al. 2019). We also collected soils along topographic gradients from depressions to uplands for biogeochemical analyses. We used multiple lines of inference to assess the drivers of spatial variation in soil C and N between the depressions vs. uplands as well as among individual cropped depressions. If recent measurements (i.e., 2017–2018) of surface water ponding correspond to long-term hydrologic conditions in these depressions, we would expect a positive relationship between ponding frequency and carbonate C. If ponding contributed to increased SOC in depression soils, then we would expect a positive relationship between ponding frequency and SOC concentration. Alternatively, if erosion was a dominant factor, we would expect strongest relationships between fine particle content and SOC, and weak or null relationships for metrics of ponding. Finally, we used stable isotope measurements to test whether depressions and uplands had similar sources of organic matter, and to indicate if crop residue inputs were contributing to SOC accrual in the depressions.

## Materials and methods

### Study area and soil sampling

The Des Moines Lobe geological region of north-central Iowa is characterized by a high density of depressional wetlands resulting from the retreat of Wisconsin-age glaciers, and most wetlands have been drained for row crop agriculture (Van Meter and Basu 2015). Soil samples were collected from agricultural fields (41.98° N, 93.68° W) in north-central Iowa in August 2018 within a 260-ha section under corn (*Zea mays*) and soybean (*Glycine max*), which have been cropped in rotation for many decades. We selected seven depressions (1.20–6.60 ha in size) and adjacent uplands for sampling (Fig. 1). These depressions are relatively typical of the Des Moines Lobe region of IA, where the areas of individual mapped depressions were 0.04–206.4 ha with a mean of 1.31 ha and median of 0.45 ha (McDeid et al. 2019). Although our study site was relatively small, the general mechanisms that we investigated here are likely to be applicable to other croplands with similar soil and hydrological characteristics in the southern Prairie Pothole Region. Agricultural management was within

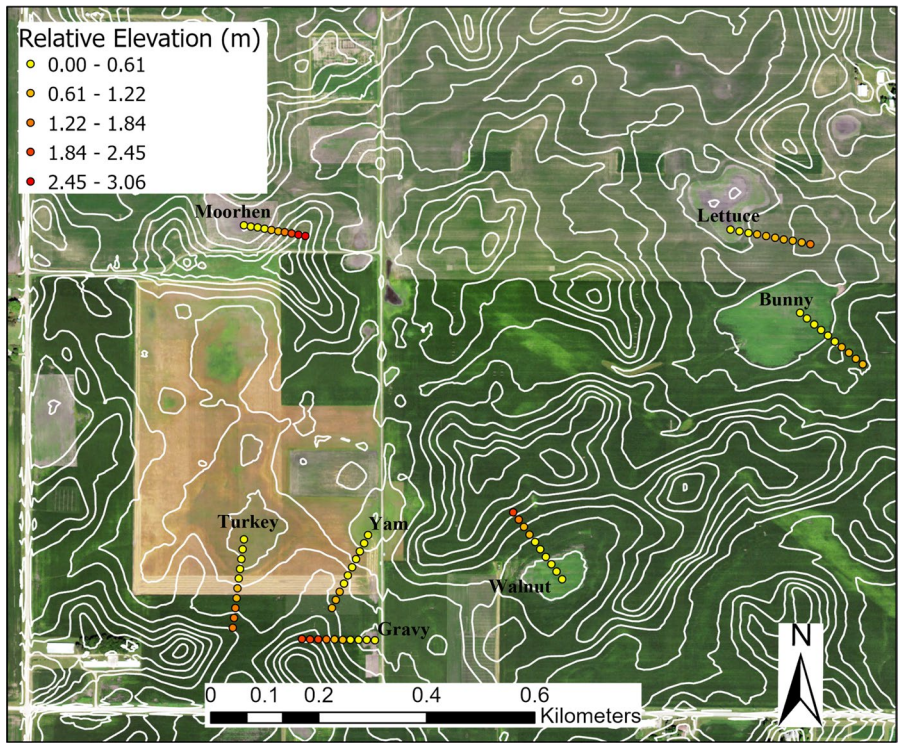


**Fig. 1** Topographic contour map showing locations of sampling plots along each depression to upland transect. Relative elevation is the elevation relative to the depression bottom in each depression. Data were obtained from United States Department of Agriculture, Farm Services Agency, National Agricultural Imagery Program, https://geodata.iowa.gov.pages/imagery, accessed on 12/10/2021 and Iowa Department of Natural Resources; https://geodata.iowa.gov/pages/two-foot-contours-county-downloads; accessed on 12/10/2021. The map was created in ArcGIS Pro 2.8.0

regional norms, with chisel plow tillage following corn and typical synthetic N fertilizer application of 168 kg N $ha^{-1}$ $year^{-1}$, with P applied as necessary according to soil test values (soybean was typically not fertilized). Crop residues were not removed, and further management details are provided by Lawrence et al. (2021). Depressions were playfully named for identification purposes based on their unique shapes, following Martin et al. (2019). Soils were formed from glacial till and developed under tallgrass prairie and wetland vegetation. The dominant soil series in the depressions include the very poorly drained Okoboji mucky silt loam (fine, montmorillonitic, mesic cumulic Haplaquolls) and Harps clay loam (fine-loamy, mixed, superactive, mesic Typic Calciaquolls). Soils near the depression boundaries include the moderately poorly drained Canisteo clay loam (fine loamy, mixed (calcareous), mesic Typic Haplaquolls), and the upland soils include the somewhat poorly drained Nicollet clay loam (fine-loamy, mixed, superactive mesic Aquic Halpudolls) and the moderately well-drained Clarion loam (fine-loamy, mixed, mesic typic Hapludolls).

These depressions pond for periods of days to weeks during most years despite the presence of subsurface drainage tile at all sites and surface inlets at some sites (Martin et al. 2019). Periods of ponding are associated with anoxic conditions, as indicated by previous measurements of reduced (Fe(II)) and oxidized iron (Fe(III)) extracted from soils by 0.5 M HCl (Yu et al. 2021). Observations of high Fe(II) during periods of high moisture indicated the presence of anoxic conditions, whereas high Fe(III) in the 0.5 M HCl extraction indicated the presence of highly reactive Fe phases formed following Fe(II) oxidation. Concentrations of Fe(II) and Fe(III) in the 0.5 M HCl extraction were also correlated with the abundance of known Fe reducing bacteria and Fe oxidizing bacteria, respectively, providing further evidence for dynamic redox cycling in these soils (Yu et al. 2021). In cases of high crop mortality in the depressions, agricultural weeds and/or native plants may establish in mid to late summer. Typical species include $C_3$ plants (e.g. *Ambrosia* spp., *Amaranthus* spp.) as well as $C_4$ plants (*Echinochloa* spp., *Setaria* spp., *Cyperus esculentus*).

We established a 125–150-m transect from the bottom of each depression to the adjacent upland, perpendicular to the topographic contour. The depression boundary was determined by the elevation data from LiDAR (Martin et al. 2019). Each transect had ten equally spaced plots (denoted positions 1–10 hereafter; 1 is the bottom and 10 is the top). The elevation of the plots was recorded from a high-resolution GPS (Trimble Geo7X, Sunnyvale, CA, USA). At each plot, we collected five 30-cm cores (2 cm diameter) within a 2-m radius. Any surface residue was removed before inserting the sampling probe, and cores were divided into depths of 0–10 cm, 10–20 cm, and 20–30 cm. Replicate cores were then composited by depth to generate spatially representative samples for each plot. Along one transect (Walnut; Fig. 1), we sampled additional cores to measure bulk density. A soil pit was dug by shovel at each plot, and a steel tube (6 cm diameter × 10 cm length) was hammered into the pit wall at the midpoint of each depth increment, and any excess soil was trimmed from the ends of the tube. Samples were quantitatively transferred from the steel tube and oven-dried at 90 °C to constant mass. Stocks of SOC along this transect were calculated as the product of SOC mass concentration and bulk density.

## Soil chemical analysis

Using air-dried and ground subsamples, we measured total C and N their $\delta^{13}C$ and $\delta^{15}N$ values with an elemental analyzer interfaced with an isotope ratio mass spectrometer (ThermoFinnigan Delta Plus XL, Waltham, MA) at Iowa State University. We measured inorganic C (hereafter referred to as carbonate C) and its $\delta^{13}C$ value using a method modified from Amundson et al. (1988) and described by Huang and Hall (2018). In brief, air-dried and ground soil subsamples (~0.25 g) were added to 120-mL glass bottles capped with butyl septa and sealed with aluminum crimps, and then flushed with $CO_2$-free air through a vent needle for 15 min at 50 mL $min^{-1}$. Two mL of 3 M HCl was added to each capped bottle using a gas-tight syringe to convert carbonate to $CO_2$. The bottles were vortexed for 30 s and then left for 24 h. We measured the $CO_2$ concentration and its $\delta^{13}C$ value by injecting 5 mL of headspace gas into a tunable diode laser absorption spectrometer (TGA200A; Campbell Scientific, Logan, UT, USA), as described in detail by Hall et al. (2017).

One caveat of the carbonate measurement method described above is that soils with negligible carbonate may release a small but detectable amount of $CO_2$

from organic matter following acid treatment. We identified and excluded these samples based on the $\delta^{13}C$ values of acid-released $CO_2$ according to the following logic. Pedogenic carbonate from deep soils (> 35 cm) has a $\delta^{13}C$ value that is 14–17‰ greater than the $\delta^{13}C$ value of $CO_2$ produced from decomposition of soil organic matter and root respiration, with negligible contribution from atmospheric $CO_2$ (Cerling et al. 1989). That is, a carbonate sample measuring −3‰ indicates a $CO_2$ source derived from organic C with a $\delta^{13}C$ value of −17 to −20‰. However, our soils were shallower (< 30 cm depth) and hence atmospheric $CO_2$ likely comprised a greater fraction of $CO_2$ in soil pores (Bowling et al. 2015). Because the $\delta^{13}C$ value of atmospheric $CO_2$ is greater than $\delta^{13}C$ of $C_3$ or $C_4$ plant biomass, mixing of atmospheric and soil $CO_2$ would lead to an even greater difference between $\delta^{13}C$ of soil respiration and $\delta^{13}C$ of soil carbonate (i.e., more positive $\delta^{13}C$ values of carbonate) then the 14–17‰ offset expected for deep soils (Cerling 1984; Cerling et al. 1989). Therefore, we defined −10‰ as the lowest plausible $\delta^{13}C$ value of carbonate in our soils, which would be consistent with a $C_3$-dominated source of respiratory $CO_2$ for carbonate formation in the conservative case with minor atmospheric mixing.

Most measured $\delta^{13}C$ values of acid-released $CO_2$ in our study were between −8 and 3‰, compatible with carbonate derived from respiratory $CO_2$ of mixed $C_3$–$C_4$ origin and a variable contribution of atmospheric $CO_2$. Several of our samples did have $\delta^{13}C$ values < −10‰ for acid-released $CO_2$, but in these cases the $CO_2$ mass released was very small (0.03–0.13 mg C $g^{-1}$, equal to 0.1–0.5% of total soil C) and soil pH was < 7, indicating that carbonate was likely negligible and that the measured $CO_2$ was actually derived from organic matter. Thus, we set carbonate C mass concentration values to zero for samples where the $\delta^{13}C$ values of acid-released $CO_2$ measured < −10‰. For each sample, SOC was then calculated by subtracting carbonate C from total soil C. The $\delta^{13}C$ value of SOC was calculated by a two-source mixing model (Huang et al. 2021):

$$\delta^{13}C_{SOC} = \frac{\delta^{13}C_{total} \times C_{total} - \delta^{13}C_{carbonate} \times C_{carbonate}}{C_{total} - C_{carbonate}}$$

Here, $\delta^{13}C_{SOC}$, $\delta^{13}C_{total}$, and $\delta^{13}C_{carbonate}$ are the $\delta^{13}C$ values of SOC, total C, and carbonate C, respectively; $C_{total}$ and $C_{carbonate}$ are the mass concentrations of soil total C and carbonate C, respectively.

Field-moist subsamples of all soils were measured for soil pH in 1:1 slurries of soil and deionized water. We measured soil particle size and oxalate-extractable metals only on air-dried 0–10 cm samples. Sand, silt and clay-sized particles were measured by sieving and sedimentation following aggregate dispersion with sodium hexametaphosphate (Kettler et al. 2001). Subsamples were extracted by ammonium oxalate at pH 3 to quantify Fe, Al and Si in short-range order phases and organo-metal complexes (Loeppert and Inskeep 1996). Specifically, 0.5 g of each soil sample was extracted in the dark with 30 mL of 0.175 M ammonium oxalate + 0.1 M oxalic acid for 2 h, and then was centrifuged at 10,000×*g* for 10 min. Metals in the oxalate extraction were measured by inductively coupled plasma optical emission spectroscopy (ICP-OES; Perkin Elmer Optima 5300 DV, Waltham, MA, USA). The oxalate extraction dissolves a highly reactive portion of soil Fe that is critically linked to SOC dynamics because these atoms may readily form complexes with organic matter, while also potentially serving as electron acceptors and donors for anaerobic microbial metabolism or abiotic reactions (e.g., Chen et al. 2020).

### Laboratory incubation

Field-moist soil sampled from all plots along four transects was incubated over 128 days to monitor soil $CO_2$ production and its $\delta^{13}C$ value. This length of incubation was chosen to improve estimation of active C turnover time (typical values are several months) by first-order models. When these samples for incubation were collected in August of 2018, the transects named Bunny and Walnut were planted to soybean, while Lettuce and Moorhen were planted to corn. Different masses of incubated soil were selected for each depth increment to maintain similar $CO_2$ accumulation in the incubation jar headspace among samples (5 g, 7.5 g, and 10 g dry mass equivalent for 0–10, 10–20 and 20–30 cm, respectively). Subsamples of fresh soil from each plot and each depth increment were gently mixed and brought to field moisture capacity after coarse roots and macrofauna were removed. Each soil sample was placed in an open 50 ml centrifuge tube and incubated in a 946-ml glass jar sealed with a gas-tight aluminum lid equipped with

butyl septa for headspace gas purging and sampling. Each sealed jar was flushed with humidified $CO_2$-free air immediately following each headspace $CO_2$ measurement, allowing cumulative quantification of $CO_2$ production and its $\delta^{13}C$ value over time (Hall et al. 2017). Headspace gas was measured every 2 weeks for the first 71 days and at approximately 4-week intervals thereafter. We measured $CO_2$ concentration and its $\delta^{13}C$ value by injecting 5 mL of gas to the tunable diode laser absorption spectrometer (Hall et al. 2017). Water was added as necessary throughout the incubation to replace moisture lost during headspace flushing.

We calculated the cumulative $CO_2$ production and its $\delta^{13}C$ value over the 128-days incubation. The cumulative $\delta^{13}C$ value of $CO_2$ was calculated as:

$$\delta^{13}C_{\mathrm{cum}CO_2} = \sum_{i=0}^{128} \delta^{13}C_{CO_2} \times F_{CO_2} \Big/ \sum_{i=0}^{128} F_{CO_2}$$

Here, $F_{CO2}$ is the flux of $CO_2$ over each sampling interval $i$.

Soil C mineralization was fit with a one-pool exponential model:

$$C_{min}(\mathrm{t}) = C \times (1 - e^{-kt}),$$

where $C_{min}(t)$ is the cumulative $CO_2$ production at time t (mg $CO_2$-C $g^{-1}$ soil), C is the active C pool (mg $CO_2$-C $g^{-1}$ soil) and $k$ is the decomposition rate constant.

We acknowledge that $\delta^{13}C$ values of respired $CO_2$ could in principle be influenced by $CO_2$ release from carbonate or carbonate formation during the incubation (Huang et al. 2020). However, factors influencing carbonate solubility such as moisture, freeze/thaw, and pH change due to $O_2$ limitation did not vary during the incubation and temporal trends in $\delta^{13}C$ values of $CO_2$ did not change abruptly, as may occur during periods of carbonate loss (Ye and Hall 2020).

## Depression inundation

Inundation depth was monitored hourly using Solinst Leveloggers (Ontario, Canada) at the bottom of each depression (except for Moorhen) during 2017 and 2018 (see Martin et al. 2019 for further details). The sensors were installed from approximately May to October. Inundation characteristics of depressions were calculated as the mean percentage of time when ponding occurred (hereafter defined as "ponding time") and the mean water depth during the period of sensor installation in each year.

## Statistical analysis

First, we tested the relationship of individual soil variables with elevation relative to the boundary of each depression using generalized additive mixed models (GAMMs). These models fit statistically optimum nonlinear relationships between predictor and response variables after accounting for the spatial correlation structure of the data. The GAMMs were fit using "mgcv" package version 1.8.28 in R (Wood 2017) to assess trends of the following variables with relative elevation: carbonate C, SOC, cumulative $CO_2$ production, the $\delta^{13}C$ values of different C pools, total N, C/N ratio, the $\delta^{15}N$ value of total N, soil particle, oxalate-extractable metals, active C pool and its decomposition rate constant. The GAMMs included a fixed effect (soil depth) and a smooth term (elevation relative to the depression boundary), with transect and plot as random effects.

To address the question of how ponding was related to carbonate C and SOC among individual cropped depressions, linear regressions were used to analyze mean values (averaged across depths and plots) for samples within the depression for each transect. The Moorhen site was not included in this analysis due to lack of inundation data. To assess predictors of SOC across all of the individual 0–10 cm samples, including depressions and uplands, we also used linear mixed models (LMMs) with the "lme4" package in R (Bates et al. 2015) to test the importance of sample location (depression vs. upland), inundation (ponding time), and geochemical predictors (including pH, silt + clay, $Fe_o$, $Al_o$ and $Si_o$) for SOC. All predictor variables were used as fixed effects except for transect, which was included as a random effect in the LMMs. The Variance Inflation Factor (VIF) was used to detect multicollinearity. Accordingly, relative elevation was not included as a fixed effect in the LMMs as it was highly correlated with other predictors. For the metrics of inundation, we only selected ponding time since preliminary comparisons showed that the model with ponding time had a lower Akaike Information Criterion (AIC) value than otherwise similar models which included mean water depth. The relative contributions and significance of the predictors in

the optimum model were determined based on standardized regression coefficient estimates and Wald chi-square test, respectively. The individual predictors with significance of $P<0.05$ were kept in the final model by using stepwise backward selection, which sequentially removed the variables with the highest $P$ values. We reported conditional $R^2$ and marginal $R^2$ of the optimum model, which represented variance explained by the model and by only the fixed effects, respectively (Nakagawa and Schielzeth 2013). The VIF values for the optimum model were all $<3$, indicating no major concern about multicollinearity. All statistical analyses were conducted with R version 3.6.1. The data were reported as mean values with standard errors.

## Results

### Topographic trends in soil C, N, and their isotopic composition

Carbonate C accounted for 0.4–53% of total soil C and significantly increased with depth ($4.3\pm0.7$ mg C $g^{-1}$ for 0–10 cm, $5.0\pm0.9$ mg C $g^{-1}$ for 10–20 cm and $5.8\pm1.0$ mg C $g^{-1}$ for 20–30 cm; $P<0.05$; Fig. 2a). Carbonate C significantly peaked near the depression boundary in samples from all depths ($P<0.01$ for GAMM smooth function; Fig. 2a). The $\delta^{13}C$ values of carbonate C did not vary with depth ($-3.1\pm0.2$‰ on average) but increased slightly with relative elevation ($P<0.01$) from $-4.7$‰ at the depression bottom to $-2.0$‰ at the top of the transects, as predicted by the GAMM (Fig. 2b). Among transects, carbonate C was highest in Lettuce ($12.7\pm2.0$ mg C $g^{-1}$), followed by Turkey ($8.4\pm1.5$ mg C $g^{-1}$), Yam ($7.3\pm1.1$ mg C $g^{-1}$), Bunny ($3.8\pm0.7$ mg C $g^{-1}$), and Walnut ($2.2\pm0.7$ mg C $g^{-1}$). As expected, soils from these transects had strongly to moderately alkaline pH values ($8.10\pm0.06$ for Lettuce, $8.14\pm0.03$ for Turkey, $8.13\pm0.03$ for Yam, $7.94\pm0.08$ for Bunny, and $7.34\pm0.12$ for Walnut). Soils from the Gravy and Moorhen transects had lower and much more variable carbonate ($0.9\pm0.3$ mg C $g^{-1}$ for Gravy and $0.1\pm0.1$ mg C $g^{-1}$ for Moorhen) and neutral to weakly acidic pH values ($6.63\pm0.16$ for Gravy and $6.88\pm0.10$ for Moorhen).

In contrast to carbonate C, SOC concentration decreased significantly with relative elevation and depth ($P<0.01$ for both; Fig. 2c), from an average of 40.2 mg C $g^{-1}$ at the depression bottom to 12.9 mg C $g^{-1}$ at the top of the transects, according to the GAMM. Among depths, SOC averaged $33.7\pm1.1$ mg C $g^{-1}$ at 0–10 cm, $32.2\pm1.1$ mg C $g^{-1}$ at 10–20 cm, and $26.5\pm1.1$ mg C $g^{-1}$ at 20–30 cm. The $\delta^{13}C$ values of SOC significantly increased from $-23.5$‰ at the depression bottom to $-17.7$‰ at the depression boundary and tended to plateau with increasing elevation ($P<0.01$; Fig. 2d), and they slightly but significantly increased with depth ($-19.4\pm0.2$‰ for 0–10 cm, $-19.3\pm0.3$‰ for 10–20 cm and $-19.1\pm0.4$‰ for 20–30 cm; $P<0.05$). Similar to SOC, total N significantly decreased with relative elevation ($P<0.01$; Fig. 2e) and depth ($2.83\pm0.09$ mg N $g^{-1}$ for 0–10 cm, $2.75\pm0.09$ mg N $g^{-1}$ for 10–20 cm and $2.18\pm0.09$ mg N $g^{-1}$ for 20–30 cm; $P<0.01$). The $\delta^{15}N$ values of total N showed a nonlinear relationship with elevation, increasing from 4.6‰ at the depression bottom to 6.6‰ near the depression boundary, and then decreasing to 5.1‰ in the upland ($P<0.01$ for the GAMM smooth function; Fig. 2f), and were slightly but significantly higher in the deeper soil layers than at the surface ($5.6\pm0.1$‰ for 0–10 cm, $5.9\pm0.1$‰ for 10–20 cm and $5.8\pm0.2$‰ for 20–30 cm; $P<0.05$). Soil C/N ratios significantly varied with soil depth ($11.9\pm0.1$ for 0–10 cm and $11.7\pm0.1$ for 10–20 cm, vs. $12.4\pm0.1$ for 20–30 cm; $P<0.01$) and peaked near the depression boundary (increased from 11.3 at the depression bottom to 12.3 near the depression boundary and then decreased to 10.3 at the top of transects; $P<0.01$ for the GAMM smooth function; Fig. 2g). In the Walnut transect, bulk density was relatively similar among plots and depths, measuring $1.28\pm0.05$ g $cm^{-3}$ at 0–10 cm, $1.23\pm0.03$ g $cm^{-3}$ at 10–20 cm, and $1.29\pm0.03$ g $cm^{-3}$ at 20–30 cm. The SOC stock for 0–30 cm ranged from 95.6 to 126.9 Mg C $ha^{-1}$ among plots on the Walnut transect, and it averaged $111\pm10$ Mg C $ha^{-1}$ overall.

### Topographic trends in soil geochemical properties and SOC decomposition

We measured sand, silt and clay particles and oxalate-extractable $Fe_o$, $Al_o$ and $Si_o$ in the 0–10 cm samples. The percentage of silt + clay significantly decreased from 89% at the depression bottom to 52% at the top of the transects ($P<0.01$; Fig. 3a).

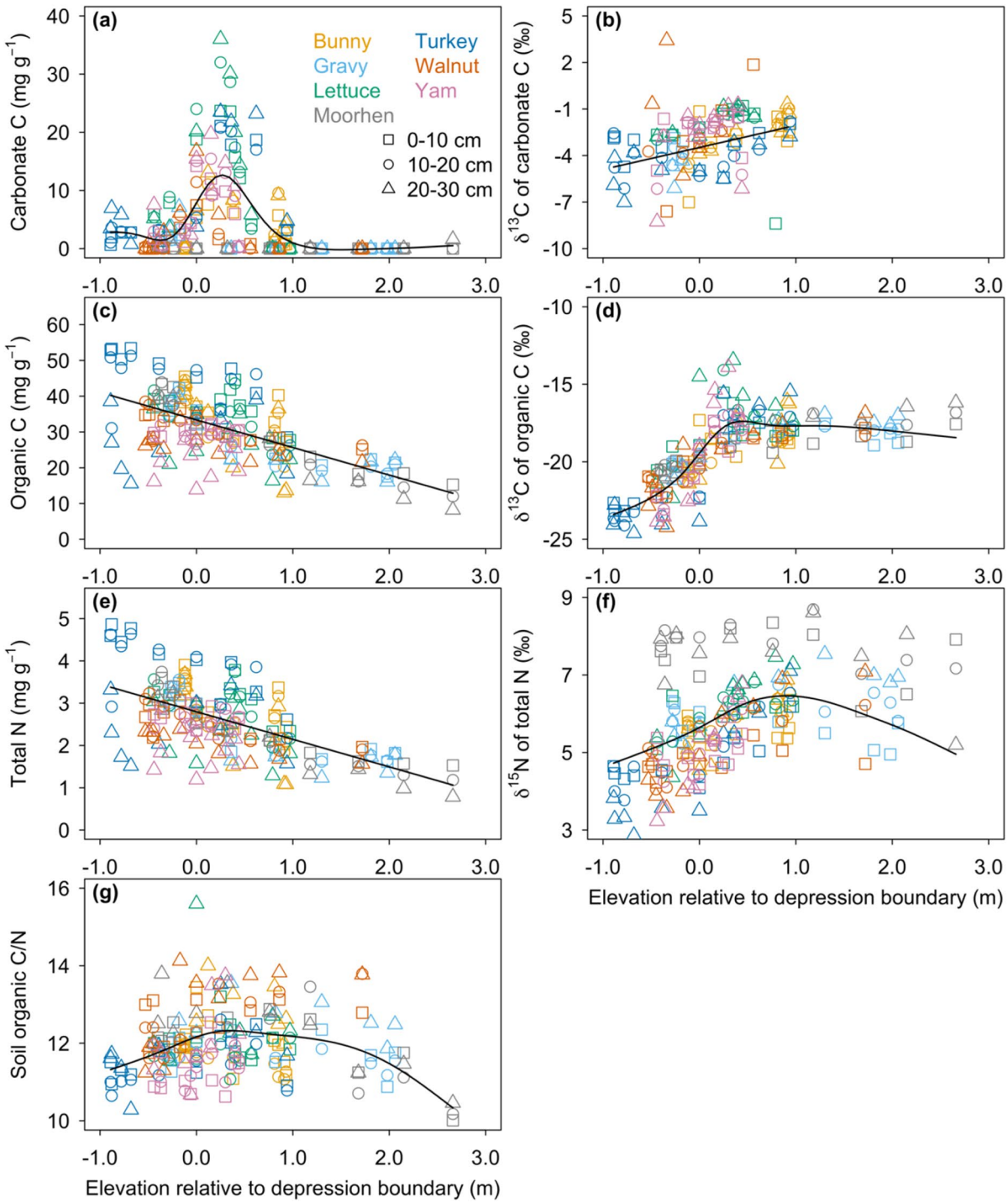


**Fig. 2** Carbonate C (**a**) and SOC (**c**), their carbon isotope values ($\delta^{13}$C) (**b**, **d**), total N (**e**) and its N isotope values ($\delta^{15}$N) (**f**) and soil C/N (**g**) plotted by elevation relative to the boundary of each depression. Lines were fit by generalized additive mixed models (GAMMs) and plotted when there was a significant trend at $P < 0.05$

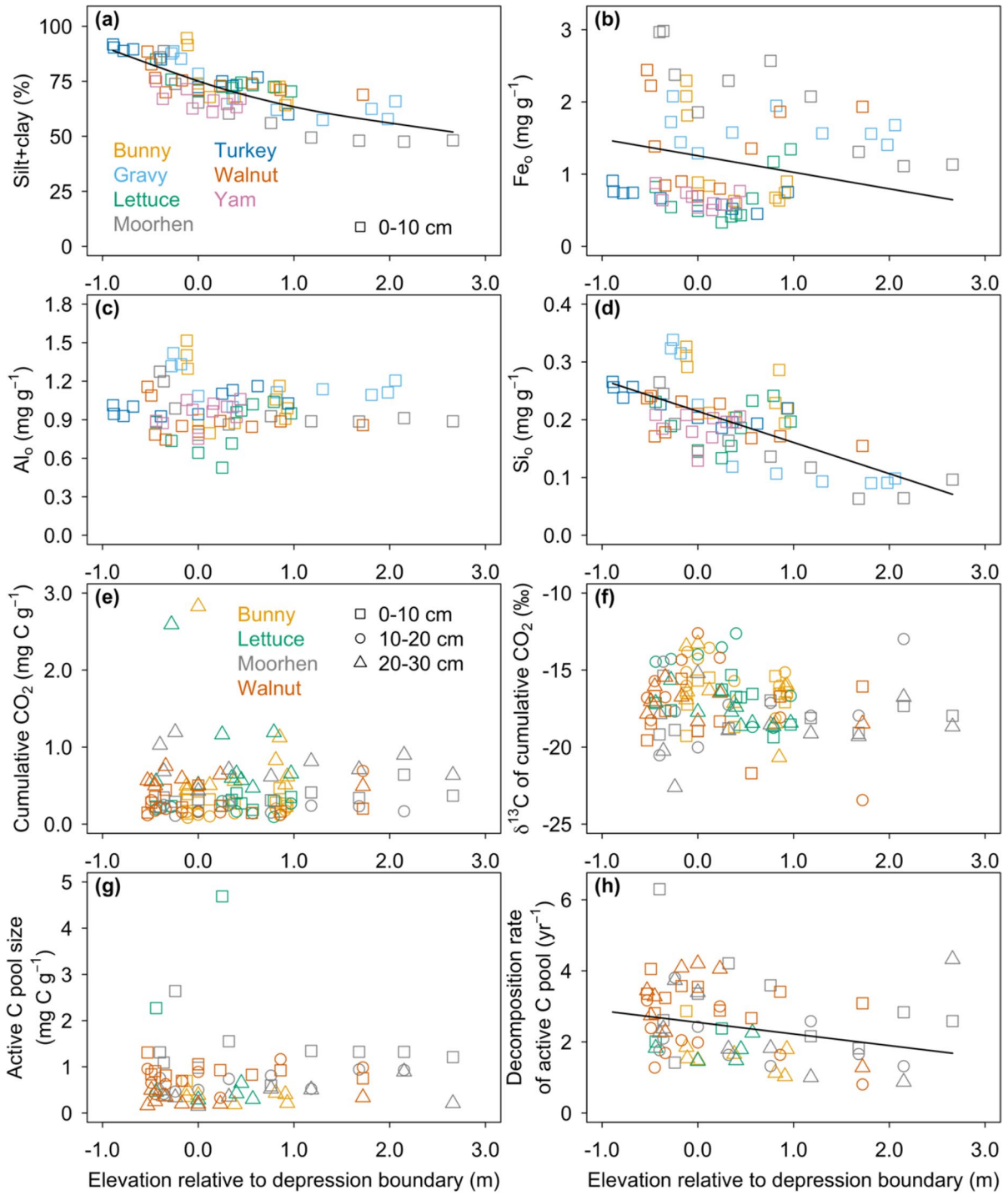


**Fig. 3** Fine particle content (**a**), oxalate-extractable Fe (**b**), Al (**c**), and Si (**d**), cumulative $CO_2$ production (**e**), cumulative carbon isotope values ($\delta^{13}C$) of $CO_2$ (**f**), active C pool size (**g**), and its decomposition rate (**h**), plotted by elevation relative to the boundary of each depression. Plotted lines indicate a significant trend at $P < 0.05$

A similar trend with relative elevation was observed for $Fe_o$, which decreased from 1.46 to 0.65 mg $g^{-1}$ ($P < 0.01$), and for $Si_o$, which decreased from 0.26 to 0.07 mg $g^{-1}$ ($P < 0.01$), but $Al_o$ did not vary consistently with relative elevation (Fig. 3a–d).

We incubated soils from four transects (Bunny, Lettuce, Moorhen and Walnut) to examine changes in soil $CO_2$ production and active C pool characteristics with relative elevation along the transects. Overall, cumulative $CO_2$ production significantly varied with soil depth and was greatest in 20–30 cm soil ($0.78 \pm 0.08$ mg C $g^{-1}$ vs. $0.30 \pm 0.02$ mg C $g^{-1}$ for 0–10 cm and $0.19 \pm 0.02$ mg C $g^{-1}$ for 10–20 cm; $P < 0.01$), but it did not vary with relative elevation (Fig. 3e). The $\delta^{13}C$ value of cumulative $CO_2$ production averaged −17.1‰ and ranged from −23.4 to −12.6‰ among all samples but did not significantly vary with soil depth or relative elevation (Fig. 3f, Supplementary Fig. S2). The active C pool calculated by the exponential model was 0.2–4.7 mg C $g^{-1}$ and the total range of decomposition rate constants was 0.8–6.3 $year^{-1}$ among soils. Both the active C pool size and the decomposition rate constant were highest in 0–10 cm soil. The active C pool size was not significantly related to relative elevation, but the decomposition rate constant of the active C pool decreased from 2.92 to 1.77 $year^{-1}$ with relative elevation as predicted by the GAMM ($P < 0.01$; Fig. 3g, h).

## Relationships of depression inundation and soil properties with soil C

Inundation characteristics of depressions were significantly related to mean carbonate C but not to mean SOC concentration in each depression, averaged from the depression bottom to the depression boundary. Mean carbonate C within each depression had strong and significantly positive relationships with ponding time ($R^2 = 0.80$; $P < 0.05$) and mean water depth ($R^2 = 0.91$; $P < 0.01$; Fig. 4a, b). However, mean SOC within each depression had no significant relationships with either the percentage of ponding time or mean water depth (Fig. 4c, d).

We used LMMs to assess the optimum predictors of SOC in 0–10 cm samples across the topographic gradients (both within and outside the depressions). Overall, there were only four significant variables remaining in the optimum model after stepwise backward selection: silt + clay, $Fe_o$, ponding time, and location (Table 1). These four predictors alone explained most of the variance in SOC concentration ($R^2_{fixed} = 0.83$), with only an additional 3% of the variance explained by the transect random effects. The optimum LMM showed that SOC was most strongly and positively related to silt + clay (Table 1). The $R^2_{fixed}$ decreased to 0.27 if silt + clay was removed from the optimum model, whereas the $R^2_{fixed}$ was 0.48 if only silt + clay was used as the fixed effect

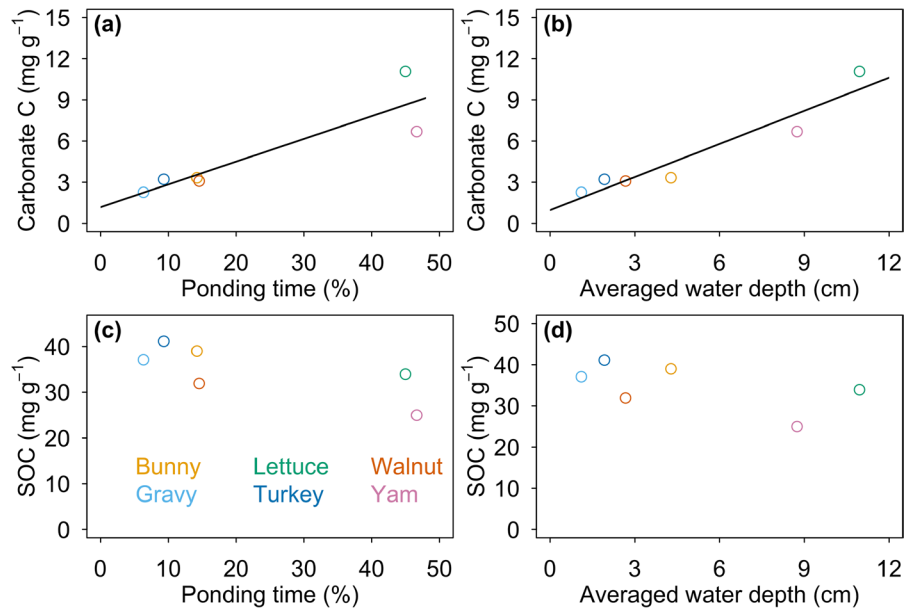


**Fig. 4** Relationships of carbonate C (**a**, **b**) and SOC (**c**, **d**) with the percentage of ponding time and mean water depth, respectively, during the growing seasons of 2017 and 2018. Each point represents C concentration averaged from the depression bottom to the depression boundary in each depression. The solid lines indicate significant relationships across all transects at $P < 0.05$ (the Moorhen site was not included due to the lack of inundation data)

**Table 1** Linear mixed model of SOC concentration in 0–10 cm samples from all seven transects (n = 70)

| Predictors | Regression coefficient | Chi-square value | P values |
|---|---|---|---|
| Silt + clay | 6.57 | 110.9 | $< 10 \times 10^{-6}$ |
| $Fe_o$ (mg $g^{-1}$) | − 3.97 | 51.8 | $< 10 \times 10^{-3}$ |
| Ponding time (%) | − 1.73 | 10.3 | < 0.01 |
| Location (depression vs. upland) | 3.2 | 5.6 | < 0.05 |
| $R^2_{fixed}$ | 0.83 | | |
| $R^2_{transect}$ | 0.03 | | |
| $R^2$ | 0.86 | | |

in the model. The high $R^2_{fixed}$ with silt + clay in the model confirmed the importance of silt + clay as the primary predictor of SOC concentration in these soils. In the optimal LMM, $Fe_o$ and ponding time were less important but had significant and negative relationships with SOC ($P < 0.01$). Location (depression vs. upland) was the least important predictor and indicated slightly but significantly higher SOC in depressions than uplands (3.2 mg C $g^{-1}$ inferred from the regression coefficient in the LMM; $P < 0.05$) after accounting for the other predictors.

## Discussion

We examined the spatial distribution of SOC and carbonate C along topographic gradients, their relationships to ponding in topographic depressions, and assessed potential biogeochemical mechanisms controlling variation in SOC concentration. Soil carbonate C was strongly related to ponding frequency measured over 2 years (Fig. 3), indicating that these ponding measurements likely represented longer-term hydrological differences among the different depressions. In contrast, SOC had no relationship with ponding frequency or depth when comparing entire depressions (Fig. 3), and at the scale of individual soil samples, the optimal statistical model showed a negative relationship between ponding frequency and SOC after accounting for other factors, as well as a negative relationship with oxalate-extractable Fe (Table 1). Although the mechanisms explaining the negative relationship between SOC and $Fe_o$ cannot be conclusively inferred with this dataset, they are consistent with the potential for Fe to stimulate organic matter decomposition during Fe reduction and oxidation (Huang and Hall 2017; Chen et al. 2020); Fe redox cycling was previously documented in all soils along the Walnut transect (Yu et al. 2021). Instead, silt + clay alone explained almost half of the variation in SOC among 0–10 cm samples. The $\delta^{13}C$ values of SOC and $\delta^{15}N$ values of bulk soil samples indicated a threshold change from lower to higher values at the depression-upland boundary, whereas $\delta^{13}C$ of respired $CO_2$ did not change with relative elevation. Together, these data support the importance of physical redistribution of SOC from uplands to lowlands via erosion of fine particles, not increased soil moisture, as the primary explanation for greater SOC concentration in these cropped depressions than in the adjacent uplands.

### Soil carbonate was strongly linked to hydrology

Distribution of carbonate C differed from SOC and appeared to be mainly associated with long-term differences in water movement. Carbonate typically peaked at the depression boundary and was greater in depressions than uplands as a consequence of accumulation and evaporation of $Ca^{2+}$-rich soil water and shallow groundwater, with greater carbonate precipitation indicating decreased infiltration relative to evaporation (Khan and Fenton 1994; Richardson et al. 1994; Logsdon and James 2014). Mean soil carbonate C in depression surface soils (0–30 cm) was strongly related to ponding frequency and mean ponding depth measured during the growing season over 2 years (Fig. 4). Carbonate leaching is closely linked to rates of long-term soil water infiltration (Egli and Fitze 2001), and given the generally high carbonate in these depressional soils (Fig. 2) it would take decades for significant carbonate depletion to occur. For example, assuming a very high carbonate leaching rate of 2 mol $m^{-2}$ $year^{-1}$, which is equivalent to 1000 mm of infiltration of water at equilibrium with calcium carbonate (Egli and Fitze 2001), removal of 10 mg carbonate C $g^{-1}$ from the top 30 cm of soil (with bulk density of 1.27 g $cm^{-3}$) would take well over a century, and these sites have likely had some form of subsurface tile drainage for at least 100 years. Therefore, the close correspondence between measured ponding and carbonate C in our study suggests that our ponding measurements were representative of longer-term hydrologic differences among these

depressions, as opposed to short-term variation due to factors such as changes in tillage management or temporary obstruction of drains (Logsdon and James 2014; Martin et al. 2019). The mean ponding time of depression soils ranged from < 10% to nearly 50% (Fig. 4), so if differences in ponding were responsible for variation in SOC among depressions, we would expect a relationship between ponding time and SOC to be detectable. Rather, we found that soil physical and chemical properties were the strongest predictors of SOC in both depressions and uplands.

## Controls on SOC accumulation in cropped depressions

We found that SOC declined consistently with relative elevation from depression bottoms to adjacent uplands (Fig. 2). A similar finding was observed at a nearby field (< 5 km from our site) under similar agricultural management, where historic orthophoto interpretation and cesium ($^{137}$Cs) inventory were used to trace erosion and accumulation of fine soil particles along topographic gradients (Li et al. 2018). In that study, SOC accumulation in the depressions was proposed to result from both soil erosion and decreased SOC decomposition in depressions due to increased moisture (Li et al. 2018), although no data were available to explicitly test the latter hypothesis. Here, we suggest that soil erosion alone could explain this pattern, according to several lines of evidence.

First of all, silt + clay (fine particle content) was the most important positive predictor of SOC (Table 1), indicating the importance of physical/chemical protection provided by fine particles for SOC persistence (Hassink 1997). These particles and associated SOC have been transported downslope by soil erosion over decadal scales as indicated by $^{137}$Cs (Li et al. 2018), leading to their accumulation in depressions (Fig. 1). One might argue that increased fine particle content could also indicate a greater abundance of anoxic microsites in depression soils due to greater water retention (Keiluweit et al. 2016), even during periods when ponding did not occur. However, sustained anoxic conditions suppress plant litter decomposition and would be expected to increase the soil C/N ratio, because litter has a higher C/N than soil organic matter (Huang et al. 2020). Rather, C/N ratios were similar between depressional and upland soils, with only a slight increase near the depression boundary (Fig. 4). We speculate that this topographic pattern in C/N might be caused by hydrologic redistribution of crop residues, which tended to accumulate in clumps near the depression boundaries as water receded following ponding events (see photo in Supplementary Fig. S3). Hydrologic transport of residues and particulate organic matter might be one mechanism contributing to the small and relatively weak SOC increase associated with depressions vs. uplands in our statistical model (Table 1), after controlling for other factors.

Furthermore, ponding had a negative relationship with SOC in our regression model (Table 1), providing additional evidence that ponding did not directly contribute to greater SOC in depressional soils. Comparison of models with and without silt + clay clearly showed that the negative relationship between ponding and SOC was not a statistical artifact. Rather, it might be explained by lower soil C input under ponding due to suppressed crop growth. Natural wetland plant communities may be highly productive even when water levels fluctuate widely, because of compensatory responses among plant species with differing tolerance for drought or flooding (van der Valk 2005). However, in cropped depressions, ponding often decreases or even eliminates crop growth (McNunn et al. 2019; Edmonds et al. 2021), and growth of non-crop plants is often suppressed by herbicide application (Supplementary Fig. S3).

Even acknowledging lower crop biomass production in depressions due to ponding, we would expect that a portion of crop residues would accumulate as SOC if elevated moisture was suppressing decomposition in depression soils. In this case, we would also expect decomposition in depression soils to increase relative to upland soils following soil disturbance and aeration, such as occurred in our soil incubation experiment. Rather, the isotope data indicate that crop C inputs did not contribute substantially to SOC in the depression soils, and the incubation data showed no difference in cumulative $CO_2$ production with relative elevation. The $\delta^{13}C$ of SOC at the depression bottoms was much more negative (−23.5‰) than expected for corn–soybean rotations, whereas $\delta^{13}C$ of upland SOC (−17.7‰) was consistent with other corn–soybean systems in our region (Huggins et al. 1998; Russell et al. 2009; Ye and Hall 2020). We did observe high $\delta^{13}C$ values of SOC along with high C/N ratios in several samples from depression boundaries (Fig. 2d), and we speculate that this might

also reflect localized accumulation of corn residues following ponding as described above (Supplemental Fig. S3).

In contrast to the large topographic difference in $\delta^{13}C$ of SOC, $\delta^{13}C$ of soil respiration did not vary with relative elevation and averaged −17.1‰ (Fig. 3f), indicating that corn and soybean residues were likely major sources of respired $CO_2$ across the topographic gradient, with possible additional contributions from a mixture of $C_3$ and $C_4$ agricultural weeds in the depression soils. In any case, the similarity between $\delta^{13}C$ of SOC and $\delta^{13}C$ of soil respiration in uplands and their large difference in depressions indicates that the current mixture of $C_3/C_4$ plant residues was not a major contributor to SOC in the depression soils. Rather, the low $\delta^{13}C$ values of SOC in the depressions indicated a likely contribution from pre-agricultural prairie SOC, which was derived mainly from $C_3$ plants. The lower $\delta^{15}N$ values of total N in the depression also indicated a more conservative N cycle consistent with a pre-agricultural organic matter source. A study at a nearby field demonstrated a strong relationship between increased cesium ($^{137}Cs$), more negative $\delta^{13}C$ values, and erosion of the Mollic epipedon, consistent with the hypothesis that SOC in the depressions was largely derived from eroded topsoil formed under prairie vegetation (Li et al. 2018).

## Conclusion and management implications

We found that variation in SOC among samples from cropped depressions and uplands could mostly be explained by fine particle content and that SOC did not increase with ponding frequency. All sites had some form of drainage infrastructure, but different depressions were ponded for < 10% to almost 50% of the growing season during the study period. These results contribute to the discussion of how current and future agricultural drainage infrastructure might influence SOC. Conversion of wetlands to croplands has markedly decreased regional SOC (Euliss et al. 2006), and further increasing the drainage efficiency of drained agricultural soils might also be expected to reduce SOC due to decreased moisture, increased oxygen availability, and increased decomposition (Kumar et al. 2014; Fernández et al. 2017; Castellano et al. 2019). However, in the case of cropped depressions which already have some form of drainage infrastructure, our results indicated that increasingly poor drainage (as reflected by increased ponding and greater carbonate C) did not correspond with greater SOC. Therefore, in cases where soils already have subsurface drainage and a long history of agricultural management, it is possible that further increasing subsurface drainage to improve crop production (Castellano et al. 2019) would not necessarily lead to greater SOC loss. On the other hand, we also predict that gaining additional SOC in these cropped depression soils would require much more purposeful management. Beyond practices typically considered for upland soils, such as reduced tillage and cover crops (Paustian et al. 2016), fields with poorly drained depressions may be good candidates for conversion to perennial bioenergy crops such as *Miscanthus* × *giganteus*, which can be more flood tolerant than grain crops and have greater belowground residue inputs (Edmonds et al. 2021), thereby promoting SOC accrual. Alternatively, cropped depressions could be restored to wetlands by obstructing tile drains and planting native species. In addition to the numerous ecosystem services that wetlands provide, this strategy that could have economic benefits for farmers given that cropped depressions often have low or negative profitability (McNunn et al. 2019; Edmonds et al. 2021) and may be eligible for conservation payment programs. Regardless of future management, our results emphasize that poor drainage characteristics and periodically high moisture do not necessarily promote ongoing SOC accrual in cropped depressions, in contrast to natural undrained wetland ecosystems.

**Acknowledgements** We thank Holly J. Curtinrich for assistance with data visualization.

**Author contributions** SJH conceived the study. All authors contributed to data collection. WH synthesized and analyzed data. WH and SJH co-wrote the manuscript with input from all authors.

**Funding** This work was supported in part by Agricultural and Food Research Initiative Grants 2018-67019-27886 and 2021-67019-33424 from the USDA National Institute of Food and Agriculture, the Iowa Nutrient Research Center, and the IOW4414 and IOW05663 Hatch projects from the USDA National Institute of Food and Agriculture.

**Data availability** Data from this study are available in the Environmental Data Initiative repository (https://doi.org/10.6073/pasta/9e6001b676a0f0efb72cd4c5d82191b6).

**Declarations**

**Competing interests** The authors have no relevant financial or non-financial interests to disclose.

## References


Amundson RG, Trask J, Pendall E (1988) A rapid method of soil carbonate analysis using gas chromatography. Soil Sci Soc Am J 52:880–883. https://doi.org/10.2136/sssaj1988.03615995005200030050x

Bates D, Mächler M, Bolker B, Walker S (2015) Fitting linear mixed-effects models using lme4. J Stat Softw 67:1–48. https://doi.org/10.18637/jss.v067.i01

Berhe AA, Barnes RT, Six J, Marín-Spiotta E (2018) Role of soil erosion in biogeochemical cycling of essential elements: carbon, nitrogen, and phosphorus. Annu Rev Earth Pl Sc 46:521–548. https://doi.org/10.1146/annurev-earth-082517-010018

Bowling DR, Egan JE, Hall SJ, Risk DA (2015) Environmental forcing does not induce diel or synoptic variation in the carbon isotope content of forest soil respiration. Biogeosciences 12:5143–5160. https://doi.org/10.5194/bg-12-5143-2015

Bridgham SD, Megonigal JP, Keller JK et al (2006) The carbon balance of north american wetlands. Wetlands 26:889–916. https://doi.org/10.1672/0277-5212(2006)26[889:TCBONA]2.0.CO;2

Castellano MJ, Archontoulis SV, Helmers MJ et al (2019) Sustainable intensification of agricultural drainage. Nat Sustain 2:914–921. https://doi.org/10.1038/s41893-019-0393-0

Cerling TE (1984) The stable isotopic composition of modern soil carbonate and its relationship to climate. Earth Planet Sc Lett 71:229–240. https://doi.org/10.1016/0012-821X(84)90089-X

Cerling TE, Quade J, Wang Y, Bowman JR (1989) Carbon isotopes in soils and palaeosols as ecology and palaeoecology indicators. Nature 341:138–139. https://doi.org/10.1038/341138a0

Chen C, Hall SJ, Coward E, Thompson A (2020) Iron-mediated organic matter decomposition in humid soils can counteract protection. Nat Commun 11:1–13. https://doi.org/10.1038/s41467-020-16071-5

Choi W-J, Kwak J-H, Lim S-S et al (2017) Synthetic fertilizer and livestock manure differently affect δ15N in the agricultural landscape: a review. Agric Ecosyst Environ 237:1–15. https://doi.org/10.1016/j.agee.2016.12.020

Edmonds P, Franz KJ, Heaton EA et al (2021) Planting miscanthus instead of row crops may increase the productivity and economic performance of farmed potholes. GCB Bioenergy 13:1481–1497. https://doi.org/10.1111/gcbb.12870

Egli M, Fitze P (2001) Quantitative aspects of carbonate leaching of soils with differing ages and climates. CATENA 46:35–62. https://doi.org/10.1016/S0341-8162(01)00154-0

Euliss NH, Gleason RA, Olness A et al (2006) North american prairie wetlands are important nonforested land-based carbon storage sites. Sci Total Environ 361:179–188. https://doi.org/10.1016/j.scitotenv.2005.06.007

Fernández FG, Fabrizzi KP, Naeve SL (2017) Corn and soybean's season-long in-situ nitrogen mineralization in drained and undrained soils. Nutr Cycl Agroecosyst 107:33–47. https://doi.org/10.1007/s10705-016-9810-1

Hall SJ, Silver WL (2015) Reducing conditions, reactive metals, and their interactions can explain spatial patterns of surface soil carbon in a humid tropical forest. Biogeochemistry 125:149–165. https://doi.org/10.1007/s10533-015-0120-5

Hall SJ, Huang W, Hammel KE (2017) An optical method for carbon dioxide isotopes and mole fractions in small gas samples: tracing microbial respiration from soil, litter, and lignin. Rapid Commun Mass Spectrom 31:1938–1946. https://doi.org/10.1002/rcm.7973

Hall SJ, Russell AE, Moore AR (2019) Do corn–soybean rotations enhance decomposition of soil organic matter? Plant Soil 444:427–442. https://doi.org/10.1007/s11104-019-04292-7

Hassink J (1997) The capacity of soils to preserve organic C and N by their association with clay and silt particles. Plant Soil 191:77–87. https://doi.org/10.1023/A:1004213929699

Huang W, Hall SJ (2017) Elevated moisture stimulates carbon loss from mineral soils by releasing protected organic matter. Nat Commun 8:1774. https://doi.org/10.1038/s41467-017-01998-z

Huang W, Hall SJ (2018) Large impacts of small methane fluxes on carbon isotope values of soil respiration. Soil Biol Biochem 124:126–133. https://doi.org/10.1016/j.soilbio.2018.06.003

Huang W, Ye C, Hockaday WC, Hall SJ (2020) Trade-offs in soil carbon protection mechanisms under aerobic and anaerobic conditions. Glob Change Biol 26:3726–3737. https://doi.org/10.1111/gcb.15100

Huang W, Wang K, Ye C et al (2021) High carbon losses from oxygen-limited soils challenge biogeochemical theory and model assumptions. Glob Change Biol 27:6166–6180. https://doi.org/10.1111/gcb.15867

Huggins DR, Clapp CE, Allmaras RR et al (1998) Carbon dynamics in corn–soybean sequences as estimated from natural carbon-13 abundance. Soil Sci Soc Am J 62:195–203. https://doi.org/10.2136/sssaj1998.03615995006200010026x

James HR, Fenton TE (1993) Water tables in paired artificially drained and undrained soil catenas in Iowa. Soil Sci Soc Am J 57:774–781

Keiluweit M, Nico PS, Kleber M, Fendorf S (2016) Are oxygen limitations under recognized regulators of organic carbon turnover in upland soils? Biogeochemistry 127:157–171. https://doi.org/10.1007/s10533-015-0180-6

Keiluweit M, Wanzek T, Kleber M et al (2017) Anaerobic microsites have an unaccounted role in soil carbon stabilization. Nat Commun 8:1771. https://doi.org/10.1038/s41467-017-01406-6

Kettler TA, Doran JW, Gilbert TL (2001) Simplified method for soil particle-size determination to accompany

soil-quality analyses. Soil Sci Soc Am J 65:849–852. https://doi.org/10.2136/sssaj2001.653849x

Khan FA, Fenton TE (1994) Saturated zones and soil morphology in a Mollisol catena of central Iowa. Soil Sci Soc Am J 58:1457–1464

Knuteson JA, Richardson JL, Patterson DD, Prunty L (1989) Pedogenic carbonates in a calciaquoll associated with a recharge wetland. Soil Sci Soc Am J 53:495–499. https://doi.org/10.2136/sssaj1989.03615995005300020032x

Krichels AH, Yang WH (2019) Dynamic controls on field-scale soil nitrous oxide hot spots and hot moments across a microtopographic gradient. J Geophys Res Biogeosci 124:3618–3634. https://doi.org/10.1029/2019JG005224

Krichels A, DeLucia EH, Sanford R et al (2019) Historical soil drainage mediates the response of soil greenhouse gas emissions to intense precipitation events. Biogeochemistry 142:425–442. https://doi.org/10.1007/s10533-019-00544-x

Kumar S, Nakajima T, Kadono A et al (2014) Long-term tillage and drainage influences on greenhouse gas fluxes from a poorly drained soil of central Ohio. J Soil Water Conserv 69:553–563. https://doi.org/10.2489/jswc.69.6.553

Lawrence NC, Tenesaca CG, VanLoocke A, Hall SJ (2021) Nitrous oxide emissions from agricultural soils challenge climate sustainability in the US Corn Belt. Proc Natl Acad Sci USA 118:e2112108118. https://doi.org/10.1073/pnas.2112108118

Li X, McCarty GW, Karlen DL et al (2018) Soil organic carbon and isotope composition response to topography and erosion in Iowa. J Geophys Res Biogeosci 123:3649–3667. https://doi.org/10.1029/2018JG004824

Loeppert RH, Inskeep WP (1996) Iron. In: Methods of soil analysis. Part 3: chemical methods. Soil Science Society of America, Madison, pp 639–664

Logsdon SD, James DE (2014) Closed depression topography harps soil, revisited. Soil Horiz 55:1–7. https://doi.org/10.2136/sh13-11-0025

Lorenz K, Lal R (2022) Incentivizing soil organic carbon management in terrestrial biomes of the United States of America. In: Lorenz K, Lal R (eds) Soil organic carbon sequestration in terrestrial biomes of the United States. Springer, Cham, pp 175–201

Martin AR, Kaleita AL, Soupir ML (2019) Inundation patterns of farmed pothole depressions with varying subsurface drainage. T ASABE 62:1579–1590. https://doi.org/10.13031/trans.13435

McDeid SM, Green DIS, Crumpton WG (2019) Morphology of drained upland depressions on the Des Moines lobe of Iowa. Wetlands 39:587–600. https://doi.org/10.1007/s13157-018-1108-4

McNunn G, Heaton E, Archontoulis S et al (2019) Using a crop modeling framework for precision cost-benefit analysis of variable seeding and nitrogen application rates. Front Sustain Food Syst 3:108. https://doi.org/10.3389/fsufs.2019.00108

Nakagawa S, Schielzeth H (2013) A general and simple method for obtaining R2 from generalized linear mixed-effects models. Methods Ecol Evol 4:133–142. https://doi.org/10.1111/j.2041-210x.2012.00261.x

Paustian K, Lehmann J, Ogle S et al (2016) Climate-smart soils. Nature 532:49–57. https://doi.org/10.1038/nature17174

Ponnamperuma FN (1972) The chemistry of submerged soils. Adv Agron 24:29–96

Reddy KR, Patrick WH (1975) Effect of alternate aerobic and anaerobic conditions on redox potential, organic matter decomposition and nitrogen loss in a flooded soil. Soil Biol Biochem 7:87–94. https://doi.org/10.1016/0038-0717(75)90004-8

Richardson JL, Arndt JL, Freeland J (1994) Wetland soils of the prairie potholes. Adv Agron 52:121–171. https://doi.org/10.1016/S0065-2113(08)60623-9

Russell AE, Cambardella CA, Laird DA et al (2009) Nitrogen fertilizer effects on soil carbon balances in midwestern US agricultural systems. Ecol Appl 19:1102–1113

Schilling KE, Dinsmore S (2018) Monitoring the wildlife, hydrology and water quality of drained wetlands of the Des Moines Lobe, northern Iowa: introduction to special feature. Wetlands 38:207–210. https://doi.org/10.1007/s13157-017-0989-y

Schilling KE, Jacobson PJ, Streeter MT, Jones CS (2018) Groundwater hydrology and quality in drained wetlands of the Des Moines Lobe in Iowa. Wetlands 38:247–259. https://doi.org/10.1007/s13157-016-0825-9

Sexstone A, Revsbech N, Parkin T, Tiedje J (1985) Direct measurement of oxygen profiles and denitrification rates in soil aggregates. Soil Sci Soc Am J 49:645–651

Silver WL, Lugo AE, Keller M (1999) Soil oxygen availability and biogeochemistry along rainfall and topographic gradients in upland wet tropical forest soils. Biogeochemistry 44:301–328. https://doi.org/10.1023/A:1006034126698

Smedema LK, Abdel-Dayem S, Ochs WJ (2000) Drainage and agricultural development. Irrig Drain Syst 14:223–235. https://doi.org/10.1023/A:1026570823692

Suriyavirun N, Krichels AH, Kent AD, Yang WH (2019) Microtopographic differences in soil properties and microbial community composition at the field scale. Soil Biol Biochem 131:71–80. https://doi.org/10.1016/j.soilbio.2018.12.024

Thaler EA, Larsen IJ, Yu Q (2021) The extent of soil loss across the US Corn Belt. Proc Natl Acad Sci USA 118:e1922375118. https://doi.org/10.1073/pnas.1922375118

van der Valk AG (2005) Water-level fluctuations in north american prairie wetlands. Hydrobiologia 539:171–188. https://doi.org/10.1007/s10750-004-4866-3

Van Meter KJ, Basu NB (2015) Signatures of human impact: size distributions and spatial organization of wetlands in the Prairie Pothole landscape. Ecol Appl 25:451–465. https://doi.org/10.1890/14-0662.1

Wood S (2017) Generalized additive models: an introduction with R, 2nd edn. CRC Press, Boca Raton

Ye C, Hall SJ (2020) Mechanisms underlying limited soil carbon gains in perennial and cover-cropped bioenergy systems revealed by stable isotopes. GCB Bioenergy 12:101–117. https://doi.org/10.1111/gcbb.12657

Yu W, Lawrence NC, Sooksa-nguan T et al (2021) Microbial linkages to soil biogeochemical processes in a poorly drained agricultural ecosystem. Soil Biol Biochem 156:108228. https://doi.org/10.1016/j.soilbio.2021.108228